[10] A. Takahashi, D. Ikeda, H. Nadanawa, Y. Okami, H. Umezawa, *J. Antibiot.* **1986**, *39*, 1041–1046.

[11] Y. Hayakawa, M. Nagakawa, H. Kawai, K. Tanabe, H. Nakayama, A. Shimazu, H. Seto, N. Otake, *J. Antibiot.* **1983**, *36*, 934–937.

[12] C. L. Stevens, R. P. Glinski, K. G. Taylor, P. Blumbergs, S. K. Gupta, *J. Am. Chem. Soc.* **1970**, *92*, 3160–3168.

[13] L. Kenne, P. Unger, T. Wehler, *J. Chem. Soc. Perkin Trans. 1* **1988**, 1183–1186.

[14] J. Weiser, M. C. Holthausen, L. Fitjer, *J. Comput. Chem.* **1997**, *18*, 1264–1281.

[15] T. Miyaki, K.-I. Numata, Y. Nishiyama, O. Tenmyo, M. Hatori, H. Imanishi, M. Konishi, H. Kawaguchi, *J. Antibiot.* **1981**, *34*, 665–674.

[16] T. Arai, Y. Takamizawa, *J. Antibiot.* **1954**, *7*, 165–168.

[17] M. D. Lee, J. K. Manning, D. R. Williams, N. A. Kuck, R. T. Testa, D. B. Borders, *J. Antibiot.* **1989**, *42*, 1070–1087.

[18] J. R. Evans, G. Weare, *J. Antibiot.* **1977**, *30*, 604–606.

[19] a) G. Eisenbrand, WO EP3285 20000412, **2000**. b) R. Hoessel, S. Leclerc, J. A. Endicott, M. E. M. Nobel, A. Lawrie, P. Tunnah, M. Leost, E. Damiens, D. Marie, D. Marko, E. Niederberger, W. Tang, G. Eisenbrand, L. Meijer, *Nat. Cell Biol.* **1999**, *1*, 60–67.

[20] Fat-free soya flour (20 g) and mannitol (20 g) were taken up in tap water (1 L). The pH was adjusted to 7.8 before sterilization.

Wet Chemistry Synthesis of *β*-Nickel Aluminide NiAl**

Helmut Bönnemann,* Werner Brijoux, Hans-Werner Hofstadt, Teyeb Ould-Ely, Wolfgang Schmidt, Bernd Waßmuth, and Claudia Weidenthaler

Owing to its extraordinary physical properties *β*-nickel aluminide NiAl is an important raw material,[1] which on the one hand has a lower density than nickel,[2] while on the other at 1638 °C[3] exhibits a significantly higher melting point than nickel (1453 °C) and aluminum (660 °C). Since a dense aluminum oxide layer is formed, even at low surface oxidation, NiAl has high thermal stability and resistance to atmospheric oxygen.[4] Owing to its high resistance towards environmental influences NiAl can be used as a Ni replacement, for example in gas turbine blades and automobile construction.[5]

The mechanical properties of NiAl are highly dependent upon the conditions of preparation and grain size.[6] Traditionally, the coarse-grained material (∅ > 1 μm), which is produced by milling[7] at 800–900 °C("mechanical alloying") is brittle at room temperature. Refining the particle diameter into the nanometer range increases ductility, strength, and hardness.[8] Thus nanocrystalline NiAl, which was produced by gas-phase condensation,[9] exhibits a considerably greater microhardness than the milled material. Mechanical alloying is associated with two significant disadvantages: 1) the particles readily agglomerate to larger units at the relatively high milling temperature, and 2) large amounts of Ni and Al remain together unalloyed.

Buhro et al.[10] have described a method for the wet chemical synthesis of NiAl by the reaction of suspended $NiCl_2$ with $LiAlH_4$ in mesitylene while refluxing under an inert atmosphere. NiAl is not formed directly during the reaction but only by subsequently heating the solid to about 550 °C. The by-products LiCl and $AlCl_3$ must be removed from the solid by sublimation at 700–750 °C, whereby a relatively coarse-grained material is obtained. Withers et al[11] reacted $NiCl_2$ with Al powder at 750 °C and after purification of the crude product from $AlCl_3$ by sublimation, obtained a Ni_3Al powder with a grain size in the micrometer range (∅ = 1.4–1.8 μm). Abe and Tsuge[12] obtained a mixture of NiAl and Ni_3Al powder by the reaction of $NiCl_2$ and $AlCl_3$ with ammonium carboxylates and subsequent heating of the resulting Ni and Al carboxylates up to 1400 °C under argon.

As early as 1955 Ziegler and co-workers described the formation of colloidal nickel in the reaction of $[Ni(acac)_2]$ (acac = acetylacetonate) with AlR_3 (R = alkyl) in solution.[13] This finding was used later by Wilke et al. to explain the „nickel effect“ in the polymerization reaction of ethene on AlR_3;[14] in this context the reactions of organonickel complexes such as $[Ni(bpy)Me_2]$ (bpy = 2,2 – -bipyridine), [Ni(cdt)] (cdt = cyclododeca-1,5,9-triene), and $[NiCl_2(PR_3)_2]$ with AlR_3 or $AlHR_2$ were also investigated. Wilke et al. concluded that in these reactions thermolabile addition compounds of nickel core complexes were formed with AlR_3 or $AlHR_2$.[14]

Repeating the Ziegler experiments in an autoclave under H_2 we obtained a black dispersion, which according to transmission electron microscopy (TEM) contained colloidal nickel [Eq. (1)] The reaction of $[Ni(acac)_2]$ with Al*i*Bu_3 gave particles with a mean diameter of ∅ = 2.8 nm. After removal of the solvent and excess $AlEt_3$ in high vacuum (HV) a hard black solid remained. By hydrogenation at 80 °C under pressure (5 MPa) we obtained from this a black powder, which according to elemental analysis contained NiAl and larger amounts of an undefined, inseparable by-product [Eq. (1)].

$$\begin{aligned}&[\mathrm{Ni(acac)_2}] + 2\,\mathrm{AlEt_3} + \mathrm{H_2} \xrightarrow{\text{toluene, } 100\,^\circ\mathrm{C}} \text{black dispersion}\\&\xrightarrow{\text{HV}} \text{black solid} \xrightarrow{\mathrm{H_2},\ 80\,^\circ\mathrm{C}} \mathrm{NiAl} + \text{by-products}\end{aligned} \tag{1}$$

The reaction of $[Ni(cod)_2]$ (cod = cycloocta-1,5-diene) with $AlEt_3$ at room temperature in a molar ratio of 1:1 in toluene under a H_2 pressure of 5–10 MPa gave a clear black-brown dispersion from which a black solid precipitates. After

---

[*] Prof. Dr. H. Bönnemann, Dr. W. Brijoux, H.-W. Hofstadt,
Dr. T. Ould-Ely, Dr. W. Schmidt, B. Waßmuth, Dr. C. Weidenthaler
Max-Planck-Institut für Kohlenforschung
Abteilung Heterogene Katalyse
Postfach 101353, 45466 Mülheim an der Ruhr (Germany)
Fax: (+49) 208-306-2983
E-mail: boennemann@mpi-muelheim.mpg.de

[**] We thank Dr. B. Tesche, B. Spliethoff, and H.-J. Bongard, MPI für Kohlenforschung, Abteilung für Elektronmikroskopie for the scanning electron microscopy (SEM) images and the transmission electron microscopy (TEM) investigations and their interpretation, S. Ruthe, MPI für Kohlenforschung, Abteilung für Gaschromatographie, for the GC analyses, and Prof. E. Dinjus, Institut für Technische Chemie, Forschungszentrum Karlsruhe, for the gas MS investigations.

1433-7851/02/4104-0599 $ 17.50+.50/0

removal of the solvent by distillation and drying under high vacuum a solid, highly air-sensitive intermediate **1** is isolated, which according to elemental analysis contains Ni and Al as well as larger amounts of hydrocarbons [Eq. (2)].

$$[\mathrm{Ni(cod)_2}] + \mathrm{AlEt_3} + \mathrm{H_2} \xrightarrow{\mathrm{RT,\ 5\,MPa}} \text{black-brown dispersion} \xrightarrow{\mathrm{HV}} \mathbf{1} \qquad (2)$$

As a qualitative GC analysis of the distilled solvent showed, complexed cod is hydrogenated to cyclooctane during the reaction; the ethyl ligand in $AlEt_3$ is converted into butane and butylcyclooctane. Ethene, ethane, butene, and hydrogen were detected in the gas phase by mass spectrometry.

Compound **1** was investigated in more detail by IR spectroscopy as well as by differential scanning calorimetry (DSC) and thermogravimetry (TG) coupled with mass spectrometry (MS). A ^1H NMR spectrum could not be recorded because of the insolubility of **1** in apolar solvents. The IR spectrum (Figure 1) clearly shows the vibrational bands of aliphatic C–H bonds in the region just below 3000 cm^{-1} as well as the deformation bands of the Al alkyl groups and the bands of the Al–C bond in the fingerprint region. In addition a band at 1591 cm^{-1} appears, which presumably originates from an Al–H vibration.

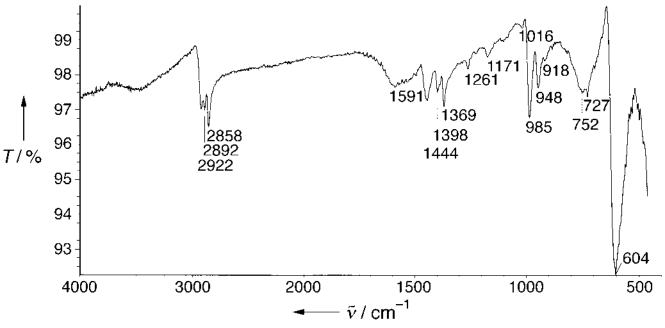

Figure 1. IR spectrum of **1**.

According to DSC/TG/MS analysis of **1** (Figure 2a, b) above a temperature of 70 °C a loss in weight occurs with release of hydrogen (*m/z* 2) and cyclooctane (*m/z* 112, 111). Signals for the C_1 to C_8 fragments are also found in this region. The cod ligand could not be detected in the sample. From above about 140 °C the formation of ethene and, in smaller amounts, ethane (*m/z* 28 and 30, respectively) occurs. Above about 200 °C methane is formed by hydrogenation of ethene (*m/z* 16, 15). Small amounts of oxygen, which occur as an impurity in the argon, react (reduction of the intensity of the signal for *m/z* 32) with hydrogen to form water (*m/z* 18); the hydrocarbons too are also oxidized to a slight extent. Up to a temperature of 400 °C the sample loses overall 7.5 wt %. A further loss in weight is observed only above temperatures of 900 °C. This loss in mass is associated with the release of lower hydrocarbons such as methane, ethene, propane, and can be attributed to the decomposition of carbon-rich hydrocarbons (coke). According to dynamic DSC/TG/MS this process is clearly still not complete at 1500 °C. The loss up to this temperature is a further 7.2 wt.% of the total mass. Thus on heating the sample up to temperatures of 400 °C under argon first hydrogen, ethene, ethane, cyclooctane, methane, and coke, which in turn partially fragments to lower hydrocarbons above 900 °C, are formed.

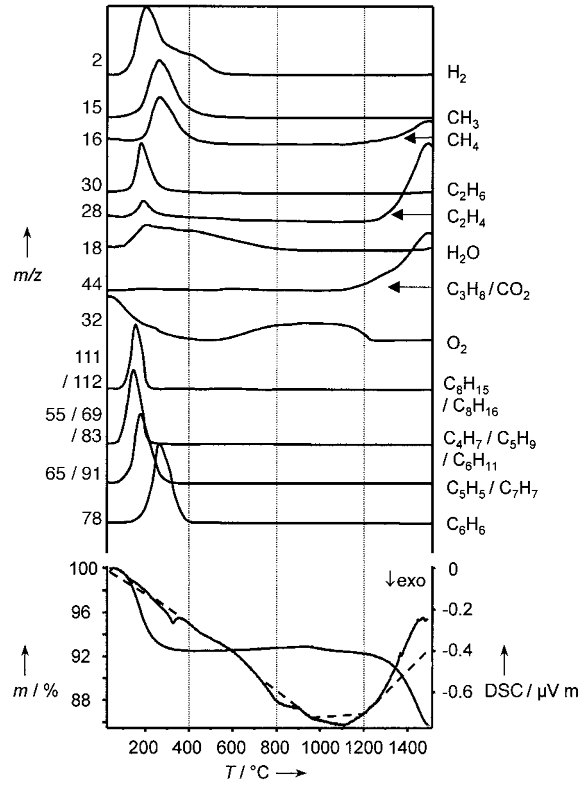

Figure 2. Top: MS curves, recorded during the TG/DSC measurement; the curves are not to scale to allow clearer presentation of lower intensities. Bottom: TG/DSC curves of **1**, measured with a heating rate of 10 °C min under argon.

The following reaction course can be proposed from the DSC/TG/MS experiments together with the IR measurements, GC analysis, and from comparison with literature data: cod is cleaved from $[Ni(cod)_2]$ which is hydrogenated to cyclooctane. $AlEt_3$ decomposes into $(AlEt_2H)_2$ and ethene, which further reacts partially to butane. To a small extent, however, cod adds to $AlEt_3$ or to AlH. The AlH species coordinates through a hydrogen bond to atomically dispersed nickel in the toluene and stabilizes this in colloidal form with formation of the black-brown toluene dispersion. [Eq. (1)]. That such a bridging bond formation is possible comes from the results of Wilke et al.[14] A Ni-H-Al bridge in $[(cdt)Ni\text{-}H\text{-}AlEt_2]$ was established directly by low-temperature ^1H NMR measurements. The broad Al–H band in the IR spectrum of the solid **1** also suggests a Ni–H–Al bridge (Figure 1). The crystal structure of $[(cdt)Ni\text{-}H\text{-}AlMe_2(C_7H_{13}N)]$ serves as a model for stabilization with hydrogen bonds.[15] In this complex Ni and Al are each tetrahedrally coordinated and are connected by an angular hydrogen bond. Because of the Al-H-Ni angle of 116° the Ni–Al distance is only about 273 pm, which is indicative of a metal–metal interaction. In agreement with the analysis and the comparative data from the literature **1** may be described as a matrix of nickel atoms coordinatively surrounded by $AlEt_2H$ (Figure 3).

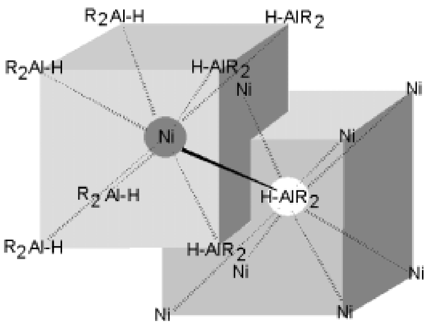

1

Figure 3. Presumed structure of the amorphous intermediate **1**.

To prepare the NiAl powder **2** compound **1** is first treated with H_2 at about 200 °C without pressure (or at a pressure of about 5 MPa). In this way the ethyl groups bonded to the Al centers are hydrogenated. Annealing at about 300 °C under an inert atmosphere finally gave with gas evolution (H_2 and C_2 hydrocarbons) almost hydrocarbon-free, high purity **2**.[16]

Compound **2** was characterized by X-ray diffraction (XRD) and scanning electron microscopy (SEM): NiAl (β-nickel aluminide: Ni content 46.6–57.7 atom %) crystallizes with a CsCl structure. The space group is *Pm3m*, the lattice parameter a ($=b=c$) is, according to the Ni fraction, 287.04 ($Ni_{46.6}Al_{53.4}$ and $Ni_{57.7}Al_{42.3}$, respectively) to 288.72 ppm ($Ni_{50}Al_{50}$).[17] In the diffractogram (Debye–Scherrer image, $Cu_{K\alpha 1}$ radiation, $\lambda = 1.540598$ Å) of **2**, reflections at $2\theta = 30.9°$, 44.4°, 54.0°, 64.7°, 71.0°, and 81.9° are observed, which supports the presence of NiAl (Figure 4).

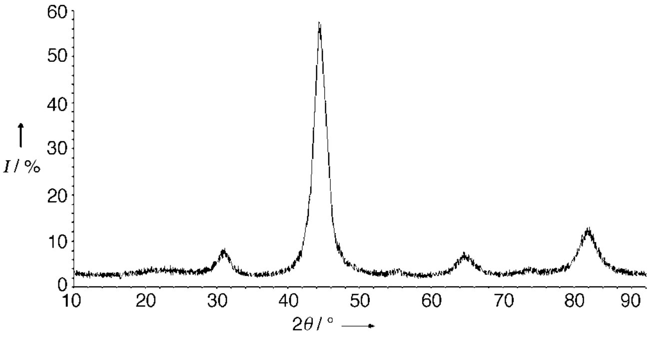

Figure 4. Powder diagram of **2** after hydrogenation and annealing at 300 °C.

To test this **2** was annealed to 1000 °C under an inert atmosphere leading to the formation of NiAl powder **3**. This gave intense, sharp reflections which can be assigned unambiguously to NiAl. In addition weak reflections of the intermetallic Ni_3Al phase (α-nickel aluminide) formed to a small extent can also be observed (Figure 5 a).

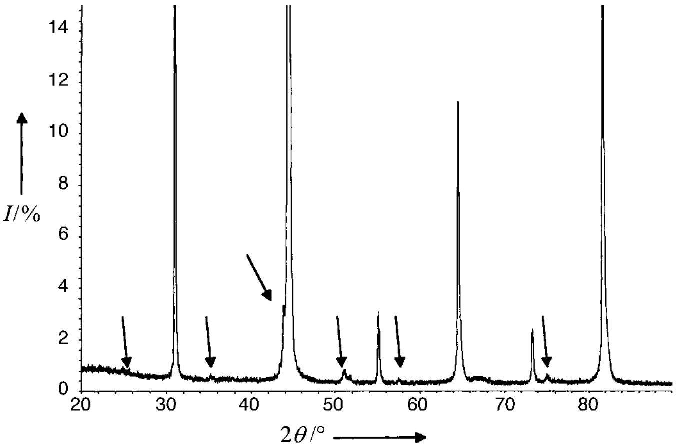

Figure 5. Section of the powder diagram of **3** after annealing at 1000 °C. The reflections of the Ni_3Al phase are indicated by arrows.

Table 1. Observed ($I_{exp.}$) and calculated (I_{calcd}) intensities in the powder diagram of **3**.

(*hkl*)	$I_{exp.}$	I_{calcd}
(100)	14	14
(110)	100	100
(111)	3	3
(200)	16	15
(210)	3	3
(211)	28	28
(220)	9	9
(300)	< 1	< 1
(221)	1	1
(310)	16	15
(311)	< 1	< 1

The measured and calculated intensities are compared in Table 1. The calculated intensities were obtained from a crystal structure refinement according to the Rietveld method.[18] The CsCl structure was used as starting model for the refinement in which the 1a position (0,0,0) was initially completely occupied with Ni, the 1b position (½,½,½) with Al. To allow for a possible disorder of Ni and Al at both positions the two positions were additionally occupied with Al and Ni, respectively. The refinement of the occupancy factors was carried out under the specification of full occupancy of both positions. The data converged for $R_B = 0.023$, $\chi^2 = 1.4\,\%$ (for all measured points) and $R_{WP} = 0.111$; the lattice parameter is 288.4(1) pm. The refinement of the crystal structure refinement gave a mixed occupancy of Ni and Al at both positions.

For the 1a position there were occupancies of 0.92(3) Ni and 0.08(3) Al. The 1b position is occupied with 0.97(2) Al and 0.03(2) Ni. This gives a composition of $Ni_{0.95}Al_{1.05}$ for the β-nickel aluminide.[19]. The evaluation of the X-ray data thus shows that **3** is a β-nickel aluminide contaminated with a small amount of α-nickel aluminide.

The particle size was determined on the basis of the data shown in Figure 4, and LaB_6 served as reference compound. The primary particle sizes were calculated according to the Scherrer method, and the (100), (110), (200), and (211) reflections were used for the calculation. A mean primary particle size of $\varnothing = 4$ nm was obtained.

The NiAl material **2** was characterized by SEM. Because of its small particle size of 2–4 nm (TEM) **2** is highly sensitive towards oxidation and was therefore annealed at 500 °C under H_2 before transfer into the SEM apparatus. The SEM image (Figure 6, original enlargement: 96 ×) of the pretreated NiAl powder shows differently sized particles (ca 150–500 µm), which have, however, no conspicuous, that is ordered,

1433-7851/02/4104-0601 $ 17.50+.50/0

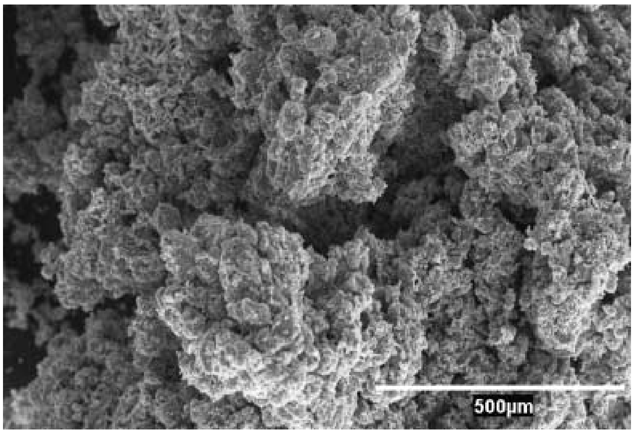

Figure 6. SEM image of **2** (after annealing at 500 °C).

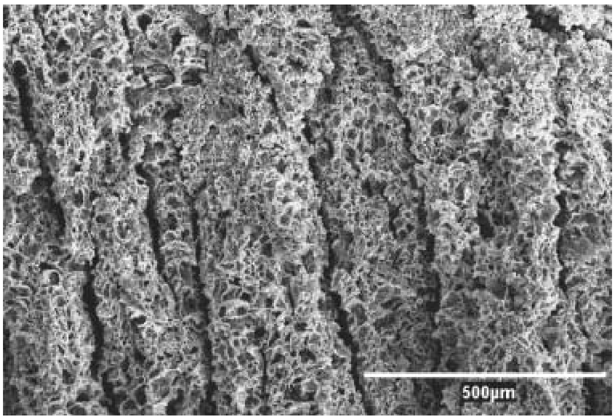

Figure 7. SEM image of **3**.

structure. The already slightly sintered NiAl powder annealed at 1000 °C exhibited, in contrast, channel-like trenches (Figure 7, original enlargement: 96 ×).

By changing the mass ratio $[Ni(cod)_2]/AlEt_3$ from 1:1 to 3:1 the synthesis described here produces α-nickel aluminide Ni_3Al. The reaction with $GaEt_3$, $[Fe(C_5H_5)(cod)]$, and $[Ce(C_{\%}H_5)_3]$ gives the ternary aluminides NiGaAl, FeNiAl, and CeNiAl (see Experimental Section).[16]

Experimental Section

Synthesis of **2**: An equimolar amount of $AlEt_3$ (3.42 g) was added to a solution of $[Ni(cod)_2]$ (8.24 g, 30 mmol) in toluene (100 mL) under an inert atmosphere. After transfer to an autoclave and pressurization with H_2 to 5–10 MPa the reaction mixture was stirred at room temperature for 72 h. A clear solution was formed from which a solid separated. After removal of the solvent and drying in high vacuum (10^{-2} Pa), the black, highly air-sensitive crude product **1** was isolated.[20] Compound **1** was hydrogenated at 200 °C and then annealed under argon at 300 °C. Elemental analysis of **2** (%): Ni 67.57, Al 30.69, C 0.02, H 0.02. Yield: 2.49 g (96.8% of the theoretical amount).

Analysis of **2**: XRD (STADI-P, Stoe, with primary monochromator): $Cu_{K\alpha 1}$ radiation (1.540598 Å), linear site-sensitive detector. The data for the Rietveld analysis were collected in the region $2\theta = 20-130°$ with an intercept length of 0.01°. The samples were measured in sealed quartz glass capillaries.

IR (Magna 750, Nicolet): KBr, resolution 4 cm^{-1}; $\tilde{\nu} = 604$vs, 727s, 752s, 918w, 948m, 985s, 1171w, 1261w, 1369w, 1389w, 1444m, 1591w, 2858m, 2892m, 2922m cm^{-1}.

DSC/TG/MS (STA 449 C, Netzsch-Gerätebau, coupled with a quadrupole mass spectrometer Thermostar 442, Balzers): measurement range 30–1500 °C, heating rate 10 °C min^{-1}, Argon.

SEM investigations were carried out with a Hitachi PC-controlled apparatus, Type S 8500 N which was equipped with an EDX detector from Oxford Instruments. For the SEM morphology investigations it was sufficient to mount the samples on a conducting carbon pad.

Synthesis of ternary aluminides as exemplified of Ga–doped NiAl **5**: $AlEt_3$ (3.09 g, 27.1 mmol) and $GaEt_3$ (1.1 g, 7 mmol) were added to a sample of $[Ni(cod)_2]$ (9.27 g, 34.07 mmol) in toluene (100 mL) under an inert atmosphere. After transfer into an autoclave and pressurization with H_2 (5 MPa), the reaction mixture was stirred for 16 h at 130 °C. After precipitation of the reaction mixture, removal of the solvent, and drying in high vacuum (10^{-2} Pa), the black, highly air-sensitive crude product **4** was isolated.[21] Product **4** was then hydrogenated for 24 h at 390 °C without pressurization to give the final product **5**. Elemental analysis of **5** (%): Ni 60.96, Al 19.89, Ga 14.40, C 0.53, H 0.08. Yield: 3.21 g (99.7% of theoretical anount).

Received: August 3, 2001 [Z 17669]

---

[1] D. B. Miracle, R. Darolia in *Intermetallic Compounds: Principles and Practise*, *Vol. 2* (Eds.: J. H. Westbrook, R. L. Fleischer), Wiley, New York, **1994**, pp. 53–72.

[2] A. Taylor, N. J. Doyle, *J. Appl. Crystallogr.* **1972**, *5*, 201–209.

[3] P. Nash, M. F. Singleton, J. L. Murray in *Phase Diagrams of Binary Nickel Alloys*, *Vol. 1* (Ed.: P. Nash), ASM International, Materials Park, **1991**, pp. 1–394.

[4] M. W. Brumm, H. J. Grabke, *Corros. Sci.* **1992**, *33*, 1677–1690.

[5] a) M. Nazmy, H.-J. Schmutzler (ABB Alstom Power AG), DE 19926669 A1, **1999** [*Chem. Abstr.* **2001**, *134*, 45499]; b) J. D. Rigney, W. S. Scott, R. Darolia, R. R. Corderman (General Electric Company), EP 0992612 A2, **1999** [*Chem. Abstr.* **2000**, *132*, 268500].

[6] M. Takeyama, C. T. Liu, *J. Mater. Res.* **1988**, *3*, 665–674.

[7] a) E. Ivanov, T. Grigorieva, G. Golubkove, V. Boldyrev, A. B. Fasman, S. D. Mikhailenko, O. T. Kalinina, *Mater. Lett.* **1988**, *7*, 51–54; b) C. Suryanarayana, F. H. Froes, *Mater. Sci. Eng. A* **1994**, *179/180*, 108–111; c) J. S. C. Jang, C. C. Koch, *J. Mater. Sci.* **1990**, *5*, 498–510.

[8] a) E. M. Schulson, *Res. Mech. Lett.* **1981**, *1*, 111–114; b) R. Bohn, T. Haubold, R. Birringer, H. Gleiter, *Scr. Metall. Mater.* **1991**, *25*, 811–816.

[9] a) S. C. Huang, A. M. Ritter, *J. Mater. Res.* **1989**, *4*, 288–293; b) T. Haubold, R. Bohn, R. Birringer, H. Gleiter, *Mater. Sci. Eng. A* **1992**, *153*, 679–683; c) H. Chang, C. J. Altstetter, R. S. Averback, *J. Mater. Res.* **1992**, *7*, 2962–2970.

[10] a) J. A. Haber, J. L. Crane, W. E. Buhro, C. A. Frey, S. M. L. Sastry, J. J. Balbach, M. S. Conradi, *Adv. Mater.* **1996**, *8*, 163–166; b) J. A. Haber, N. V. Gunda, W. E. Buhro, *J. Aerosol Sci.* **1998**, *29*, 637–645; c) W. E. Buhro, J. A. Haber, B. E. Waller, T. J. Trentler, R. Suryanarayanan, C. A. Frey, S. M. L. Sastry, *Polym. Mater. Sci.* **1995**, *73*, 39–40; d) J. A. Haber, W. E. Buhro, *J. Am. Chem. Soc.* **1998**, *120*, 10847–10855.

[11] J. C. Withers, H.-C. Shiao, R. O. Loutfy, P. Wang, *JOM* **1991**, *43*, 36–39.

[12] O. Abe, A. Tsuge, *J. Mater. Res.* **1991**, *6*, 928–934.

[13] K. Ziegler, E. Holzkamp, H. Breil, H. Martin, *Angew. Chem.* **1955**, *67*, 541–547.

[14] K. Fischer, K. Jonas, P. Misbach, R. Stabba, G. Wilke, *Angew. Chem.* **1973**, *85*, 1002–1012; *Angew. Chem. Int. Ed. Engl.* **1973**, *12*, 943–953.

[15] K. Pörschke, Habilitationsschrift, Universität Düsseldorf, **1988**, p. 86.

[16] H. Bönnemann, W. Brijoux, H.-W. Hofstadt (Studiengesellschaft Kohle mbH), German Patent Application Nr. 10123766.9, **2001**.

[17] R. D. Noebe, R. R. Bowman, M. V. Nathal in *Physical Metallurgy and Processing of Intermetallic Compounds* (Eds.: N. S. Stoloff, V. K. Sikka), Chapman & Hall, Boca Raton, **1996**, pp. 212–296.

[18] Structure refinement was carried out with the program *FullProf2000*. J. Rodríguez-Carvajal in *Abstracts of the Satellite Meeting on Powder Diffraction of the XV Congress of the IUCr*, Toulouse, **1990**, p. 127.

[19] A refinement of the crystal structure with a complete arrangement of Ni at the 1a position and Al at the 1b position gave a significantly

worse R_B value of 0.054. The secondary phase Ni_3Al was also considered in the refinement. Further details on the crystal structure investigation may be obtained from the Fachinformationszentrum Karlsruhe, 6344 Eggenstein-Leopoldshafen, Germany (fax: (+49)7247-808-666); e-mail: crysdata@fiz-karlsruhe.de), on quoting the depository number CSD-412238.

[20] Elemental analysis of **1** (%): Ni 50.65, Al 23.73, C 18.30, H 4.32. GC analysis of the condensed solution (%): butane 0.016, methylcyclohexane (hydrogenation product of toluene), 3.23, cyclooctane 2.00, butylcyclooctane 0.018, in addition 57 non-identified products with together 0.68%; residual toluene. Measurement apparatus: Carlo-Erba 4100 gas chromatograph, RTX-1 column (60 m); carrier gas H_2.

[21] Elemental analysis of **4** (%): Ni 59.7, Al 21.8, Ga 13.8, C 6.7, H 0.9.

7-Deaza-2′-deoxyxanthosine Dihydrate Forms Water-Filled Nanotubes with C−H···O Hydrogen Bonds[**]

Frank Seela,[*] Thomas Wiglenda, Helmut Rosemeyer, Henning Eickmeier, and Hans Reuter[*]

Inspection of an assembly of 7-deaza-2′-deoxyxanthosine dihydrate ($1\cdot 2H_2O$) molecules[1] within a crystal discloses interesting structural features: Besides an intramolecular hydrogen bond (N3−H···OH−5′), an array of further hydrogen bonds stabilizes a supramolecular aggregate of four molecules of **1**. This arrangement results in the formation of an almost flat tetramer (Figure 1) with an oval cavity of approximate dimensions 9.5 × 6.5 × 3.0 Å (±0.5 Å). A pile of completely stacked teramers forms a columnar nanotube-like structure (Figure 2).

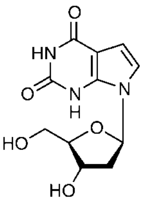

1

The synthesis of **1**[2] was performed as described previously.[3] It was crystallized from *i*PrOH/H_2O/MeOH (3/1/1), which was slightly acidified with glacial acetic acid, as a dihydrate in the monoclinic space group $P2_1$ (see Supporting Information).[4] The structure shows that **1** exists in the 2,4-dioxo form in the solid state (Figure 3); both oxo substituents lie slightly out of the ring plane.

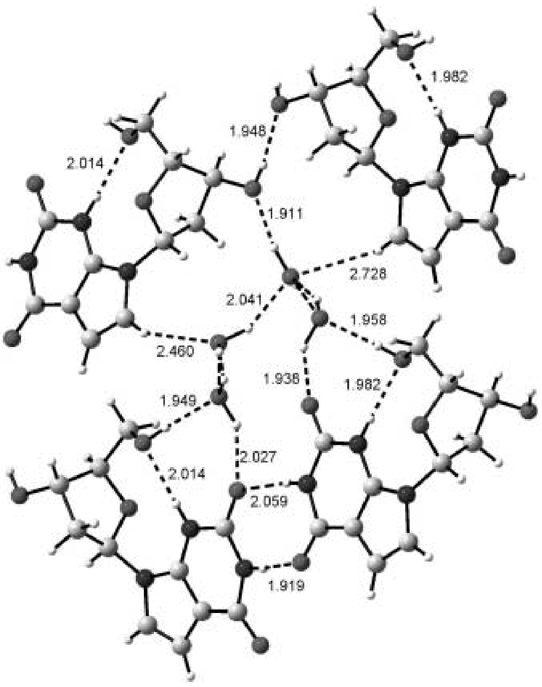

Figure 1. Length of the hydrogen bonds in a water-containing tetramer of **1**.

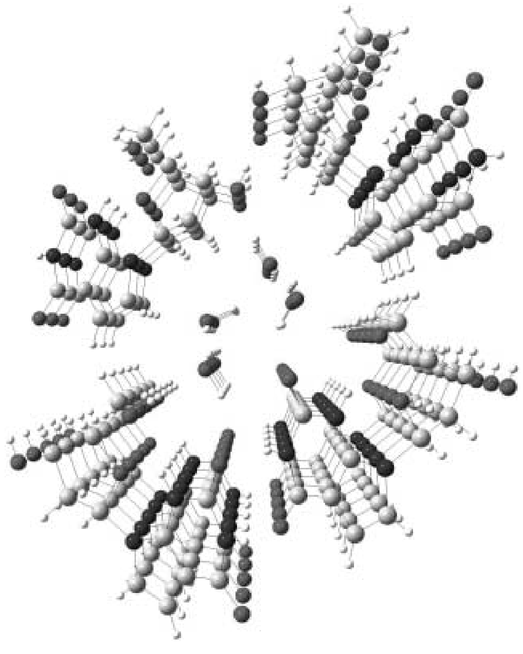

Figure 2. Nanotube of stacked tetramers (see Figure 1).

The torsion angle χ^1 (O4′-C1′-N9-C4),[5] which defines the orientation of the base relative to the sugar group (*syn*/*anti*), amounts to 61.9°; thus the nucleoside **1** adopts the *syn* conformation. A literature survey[6] of nearly 300 X-ray structures of nucleosides reveals that **1** belongs to the minor group of about 50 structures showing this N-glycosylic *syn* conformation. The *syn* conformation around the N-glycosylic bond is unusual for 7-deazapurine nucleosides.[7] In the case of **1** it is fixed by an intramolecular hydrogen bond between the H atom on N3 and the O atom of the 5′-OH group (separation 1.98 Å)[8] forcing the exocyclic 5′-CH_2OH moiety into the +sc[(+)*g*]) conformation with a torsion angle γ of 52° for C3′-C4′-C5′-O5′. The sugar ring adopts the ${}^{2'}T_{3'}$ ("south") con-

---

[*] Prof. Dr. F. Seela, Dipl.-Chem. T. Wiglenda, Dr. H. Rosemeyer
Laboratorium für Organische und Bioorganische Chemie
Institut für Chemie, Universität Osnabrück
Barbarastrasse 7, 49069 Osnabrück (Germany)
Fax: (+49)541-969-2370
E-mail: Frank.Seela@uni-osnabrueck.de

Prof. Dr. H. Reuter, H. Eickmeier
Anorganische Chemie II
Institut für Chemie, Universität Osnabrück
Barbarastrasse 7, 49069 Osnabrück (Germany)
Fax: (+49)541-969-3323
E-mail: hreuter@uni-osnabrueck.de

[**] Financial support from the Deutsche Forschungsgemeinschaft is gratefully acknowledged.

Supporting information for this article is available on the WWW under http://www.angewandte.com or from the author.